

# A Method to Determine Fuel Transport Dynamics Model Parameters in Port Fuel Injected Gasoline Engines During Cold Start and Warm-Up Conditions

**M. Shahbakhti**

Department of Mechanical Engineering,  
University of Alberta,  
Edmonton, AB, T6G 2G8, Canada

**M. Ghafari**

**A. R. Aslani**

**A. Sahraeian**

Iran Khodro Engine Research, Design, and Manufacturing  
Company (IPCO),  
Tehran, 11369, Iran

**S. A. Jazayeri**

**S. Azadi**

Department of Mechanical Engineering,  
K. N. T. University of Technology,  
Tehran, 19991 4334, Iran

*In order to meet stringent emission standards, it is essential to have a precise control of air-fuel ratio (AFR) under cold start and warm-up conditions. This requires an understanding of the fuel transport dynamics in the intake system during these conditions. This study centers on estimating the parameters of a fuel transport dynamics model during engine operation at different thermal conditions ranging from cold start to fully warmed-up conditions. A method of system identification based on perturbing fuel injection rate is used to find fuel dynamics parameters in a port fuel injected (PFI) spark ignition engine. Since there was no cold chamber available to prepare cold start conditions, a new method was utilized to simulate cold start conditions. The new method can be applied on PFI engines, which use closed valve injection timing. A four-cylinder PFI engine is tested for different thermal conditions from  $-15^{\circ}\text{C}$  to  $82^{\circ}\text{C}$  at a range of engine speeds and intake manifold pressures. A good agreement is observed between simulated and experimental AFR for 52 different transient operating conditions presented in this study. Results indicate that both fuel film deposit factor ( $X$ ) and fuel film evaporation time constant ( $\tau_f$ ) decrease with increasing coolant temperature or engine speed. In addition, an increase in the intake manifold pressure results in an increase in  $X$  while causes a decrease in  $\tau_f$ .*  
[DOI: 10.1115/1.4000150]

## 1 Introduction

Over 80% of the total CO and HC emissions in standard driving cycles are generated during the cold phase when cars start at an

ambient temperature of  $20^{\circ}\text{C}$  [1,2]. Results of a study [2] in Europe indicate that about 35% of cars are usually started in cold conditions and about one third of all travels are completely done within the warm-up period. Precise control of air-fuel ratio (AFR) is one of the major solutions to tackle the problem of high emission in cold start conditions [3]. However, precise AFR control during cold start is a challenging problem and is highly dependent on the characterization of the fuel transport mechanism in an engine.

Early works on characterizing fuel transport dynamics were carried out by Rasmussen [4] and later by Aquino [5], and Hires and Overington [6]. They proposed a simple phenomenological model to explain fuel transport characteristics. Although many models have been proposed later [7–10], the model of Aquino has been used in numerous studies [11–15] because of its good accuracy and simplicity, which are desirable for control applications. The model of Aquino assumes that a fraction ( $X$ ) of the fuel delivered to the intake system is deposited as fuel film on the wall surfaces, and then the fuel leaves the wall film at the rate proportional to the mass of the fuel in the film and inversely proportional to a time constant  $\tau_f$ . The most common method to identify  $X$  and  $\tau_f$  is to apply AFR excursions by changing the injected fuel or throttle position and record the AFR response by sampling the exhaust gas stream. This method for identification of  $X$  and  $\tau_f$  has been used in different studies [15–17]. In these studies, a cold chamber with adjustable preconditioning room temperature is used to identify  $X$  and  $\tau_f$  in cold start conditions. The cost of this climatic chamber and its maintenance requirements impose a high expense on identification tests for cold start conditions. A climatic chamber is not available to us, thus a new method is designed to prepare for cold start tests. The primary aim of this study is to establish a technique to determine  $X$  and  $\tau_f$  for a test engine at different working conditions, particularly the cold phase.

## 2 Model Description

**2.1 Fuel Transport Model.** The injected fuel mass flow rate  $\dot{m}_{fi}$  divides into two parts: a vapor phase mass flow  $\dot{m}_{fv}$  and a liquid phase mass flow  $\dot{m}_{fl}$ . The portion of the fuel which goes into the liquid phase is denoted as  $X$  ( $0 \leq X \leq 1$ ) while the remaining portion ( $1-X$ ) is entrapped into the air stream as vapor. The time constant  $\tau_f$  describes the mean evaporation time for the fuel film flow at the intake ports. The governing equations are [18]

$$\dot{m}_f = \dot{m}_{fv} + \dot{m}_{ff} \quad (1)$$

$$\dot{m}_{fv} = (1-X)\dot{m}_{fi} \quad (2)$$

$$\dot{m}_{ff} = \frac{X\dot{m}_{fi} - \dot{m}_{ff}}{\tau_f} \quad (3)$$

where  $\dot{m}_{ff}$  represents the fuel mass flow rate coming from the fuel film and  $\dot{m}_f$  is the resulting fuel mass flow rate inducted into the cylinder. Similar to Refs. [14,19], a pure time delay ( $\Delta T$ ) is considered for the time period between the moment of charge induction into the cylinder and the moment of AFR measurement by a universal exhaust gas oxygen (UEGO) sensor. The UEGO sensor is modeled as a lag element to estimate the time response from the sensor [14,19,20]. Relation (4) indicates the transfer function for the process from injecting fuel until AFR measurement by the UEGO sensor

$$\frac{\dot{m}_{f_{\text{UEGO}}}(s)}{\dot{m}_{fi}(s)} = \frac{1 + \tau_f(1-X)S}{1 + \tau_f S} \times e^{-s\Delta T} \times \frac{1}{1 + \tau_{\text{UEGO}}S} \quad (4)$$

where  $\dot{m}_{f_{\text{UEGO}}}$  is the fuel mass flow rate measured by the UEGO sensor and  $\tau_{\text{UEGO}}$  is the sensor time constant. A method of system identification using fuel perturbation will be used to find  $X$ ,  $\tau_f$ , and  $\Delta T$  for different operating conditions.

Manuscript received May 11, 2009; final manuscript received May 23, 2009; published online April 26, 2010. Editor: Dilip R. Ballal.

**Table 1 Conditions of cold start and warm-up tests**

Engine state	$T_{\text{coolant}}$ (°C)	$P_{\text{manifold}}$ (kPa)	Engine speed (rpm)
Cold start	10, 0, -8, -15	50, 60	1700, 2255
Warm-up	30, 45, 60, 82	44, 60, 73	1700, 2255, 3680

### 3 Experimental Setup

Experiments are carried out on a locally manufactured engine called Paykan, which is a four-cylinder port fuel injected (PFI) engine with a displacement volume of 1598 cc and a compression ratio of 8.5:1. The engine uses an injection pressure of 3 bar and the cone angle of injectors is 13 deg. The UEGO sensor is located at a distance of about 73 cm from the exhaust manifold, near the place of coincidence of exhaust gases from all cylinders. AFR values are measured by HORIBA (Kyoto, Japan) Mexa-700 $\lambda$  gas analyzer, which has a response time of about 0.1 s. The accuracy in measuring  $\lambda$  (i.e., AFR/AFR<sub>stoich</sub>) is 0.02 for rich mixtures and 0.007 for stoichiometric mixtures. The engine speed is measured by a tachometer with an accuracy of  $\pm 1$  rpm and the intake manifold absolute pressure is measured by manifold absolute pressure (MAP) sensor with an accuracy of about 1%. All temperatures are measured by *K*-type thermocouples with an accuracy of  $\pm 0.5^\circ\text{C}$ .

**3.1 Test Procedure.** Main factors influencing fuel dynamics parameters are coolant temperature, intake manifold pressure (engine load), and engine speed. Thus, the engine is set for a range of operating conditions listed in Table 1. Values in Table 1 are based on the break points in the base injection map of the engine control unit (ECU) for the Paykan engine.

A rectangular air-fuel excursion is made using a rectangular fuel injection rate at a constant air flow rate and the engine air-fuel equivalence ratio ( $\Phi$ ) is measured by the UEGO sensor. Thresholds of  $\Phi$  excursion are chosen depending on the engine's operating condition.  $\Phi$  thresholds of  $\langle\langle 1.1$  and  $1.4 \rangle\rangle$  are used for cold start tests,  $\langle\langle 1$  and  $1.25 \rangle\rangle$  for warm-up tests ( $20$ – $60^\circ\text{C}$ ), and  $\langle\langle 0.9$  and  $1.1 \rangle\rangle$  for fully warmed-up tests ( $+82^\circ\text{C}$ ). The frequency of  $\Phi$  excursions is chosen by using the system step response and it ranges from 0.1 Hz to 1 Hz for the tests done in this study.  $\Phi$  values are measured by sampling frequency of 100 Hz.

In warm-up tests, a controllable valve equipped with a proportional, integral, differential (PID) controller adjusts hot water flow rate into a cooling heat exchanger to obtain a desirable engine inlet coolant temperature. Then, the injection pulse width is determined to get desirable  $\Phi$  thresholds. Finally, a rectangular input  $\Phi$  is implemented and the system response (engine out  $\Phi$ ) is recorded by the UEGO sensor. Water is used as the engine coolant and fuel temperature is between  $25^\circ\text{C}$  and  $30^\circ\text{C}$ . In contrast with warm-up tests, conditions in cold start tests are more difficult to prepare. To simulate cold start, the engine needs special preconditioning. The engine should be kept in a cold chamber for a certain time period according to automotive test standards. Since there is no cold chamber available to us, the following method is used.

Detailed studies [21–23] show that air temperature has a very limited influence on fuel droplets and liquid fuel film evaporation. Although heat transfer from air to fuel droplets increases as air temperature increases, an increase in intake port fuel film vapor generation is almost negligible [21]. Using the results in these studies, it can be concluded that if it is not possible to provide cold air at a desirable temperature, there will be an acceptable error in the estimation of fuel dynamics parameters. Also, fuel is injected into the intake ports and the injection timing is based on closed valve injection in the Paykan engine. Thus, the most effective factor on fuel film evaporation rate is the wall temperature of the intake port. If the intake port wall temperature is the same as

the engine's cold start temperature, there will be a good approximation of cold start condition, so fuel dynamics parameters can be estimated for similar cold start conditions. The most effective factor on the intake port wall temperature is the coolant temperature. The following process is done to ensure that the intake port wall reaches the desirable temperature.

The equipment used for cold start tests is shown in Fig. 1. As illustrated a subzero portable chiller is used to provide 900 liters of coolant (50% water+50% Ethylen Glycol) at the desirable temperature ( $+10^\circ\text{C}$  to  $-15^\circ\text{C}$ ) and the coolant is stored in an insulated tank. Then a centrifugal pump is used to circulate the coolant with a constant mass flow rate of 25 l/min in a stalled engine for a certain time. A lumped thermal model [3,24] is used to determine the time necessary for coolant circulation in the stalled engine to ensure that the intake port walls have reached the desirable temperature. The calculated time is tested on the experimental engine by monitoring the difference between inlet and outlet coolant temperatures for the stalled engine. If the calculated time is not enough, coolant is circulated for an extra time until the inlet and outlet coolant temperatures are the same. A heat exchanger, as shown in Fig. 1, is used to ensure that fuel has the required temperature for each cold start test. Using this heat exchanger, there is a maximum of  $1$ – $2^\circ\text{C}$  deviation from the desirable temperatures. Once the cold start test is over, the engine is run toward the fully warmed-up condition in preparation for the next test. This helps to avoid the condition where the engine performance is affected by a previous test since there is a high possibility of soot formation around the spark plug vicinity when running the engine with rich mixture in cold start conditions.

### 4 Results

Once the experimental data are collected, methods of system identification [25] are used to identify both  $\Delta T$  and fuel dynamics parameters ( $X, \tau_f$ ) for the operating conditions in Table 1. Measured and simulated  $\Phi$  for two different thermal operating conditions is shown in Fig. 2 and indicates a good agreement between measured and predicted  $\Phi$ . Figures 3 and 4 indicate the values of identified  $X$  and  $\tau_f$  versus variations in engine coolant temperature, engine speed, and intake manifold pressure in cold start and warm-up conditions. As seen in the figures,  $X$  and  $\tau_f$  decrease as the coolant temperature increases. This is caused by changes in heat energy input at the intake port walls and also to air-borne fuel droplets when coolant temperature varies. With a higher coolant temperature, the corresponding temperature at the intake port walls and the inducted air into the cylinder will be higher. In addition, the fuel film transport to cylinders increases due to reduced viscosity of the fuel film at higher intake port wall temperatures.

Results in Figs. 3 and 4 show a decrease in  $X$  and  $\tau_f$  with increasing engine speed. When engine speed increases, there will be higher mixing and drag forces on air-borne droplets that promote fuel vaporization and reduce fuel deposition. Thus,  $X$  decreases with increasing engine speed. Decrease in  $\tau_f$  with increasing engine speed is due to having more heat flux at the intake port walls at higher engine speeds, which leads to an increase in temperature at the intake port walls [22]. In addition, mean air velocity at the intake ports of the Paykan engine increases from 24.5 m/s to 59 m/s when increasing the engine speed from 1700 rpm to 3680 rpm [3]. This promotes higher fuel film velocities, liquid entrainment, and mass transfer into the cylinder.

When the intake manifold pressure increases,  $X$  increases but  $\tau_f$  drops, as shown in Figs. 3 and 4. Obtaining higher  $X$  at higher intake pressures can be explained by having enhanced evaporation at lower air pressures [21]. To explain the reduction in  $\tau_f$  by increasing intake pressure, three factors should be considered. The most dominant factor is that more charge is inducted into the cylinder at higher intake pressures; thus, the heat energy flux at the intake port walls increases, and eventually, there will be an

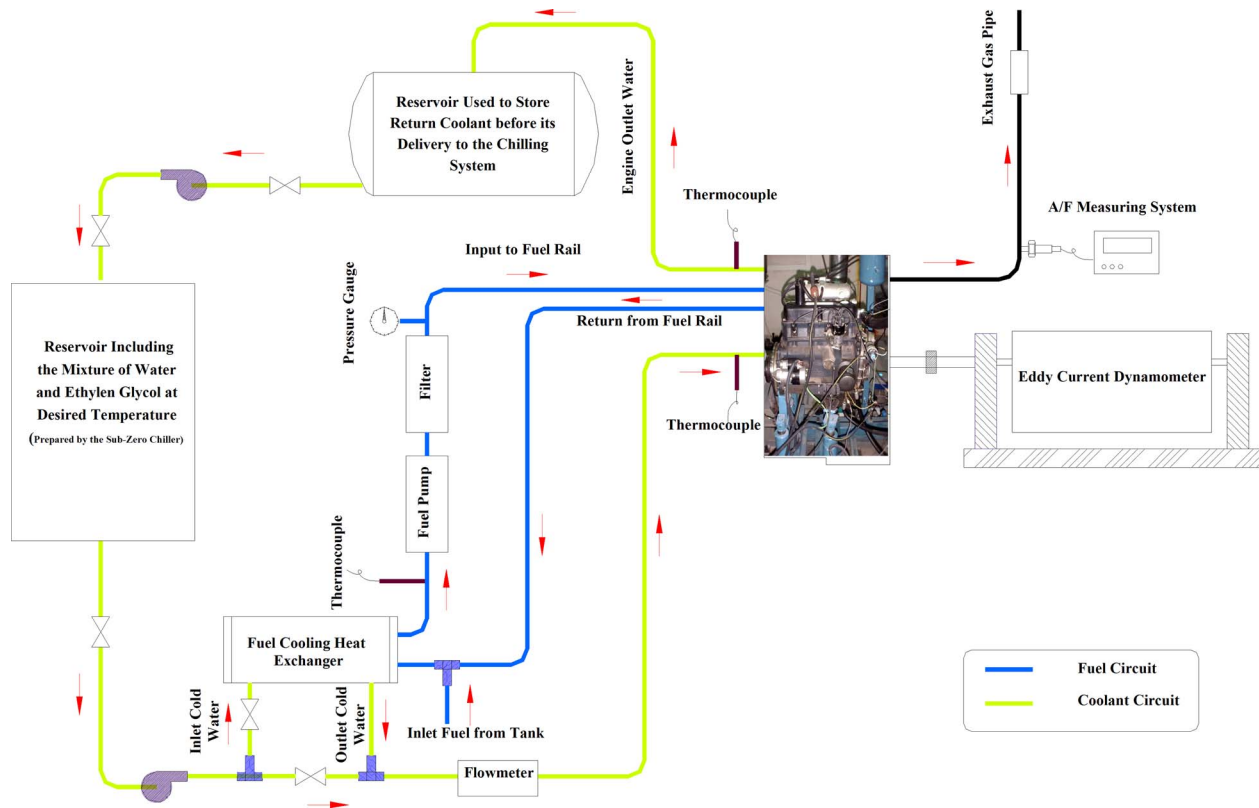


Fig. 1 Schematic of the system used in cold start tests

increase in temperature at the intake port walls [22]. This leads to more fuel film evaporation. The second factor is an increase in air velocity at the intake valve vicinity with increasing intake manifold pressure [26], which results in more fuel film evaporation and liquid entrainment. The last factor is that a lower air pressure promotes higher fuel film evaporation. All together with increasing intake manifold pressure, the first and second factors cause a decrease in  $\tau_f$ , while the third factor causes an increase in  $\tau_f$ .

Comparing the magnitude of influence on  $X$  and  $\tau_f$  by changing the main engine variables discussed for the Paykan engine, the following trend can be observed.

←  
 More influence on  $\tau_f$   
 $T_{\text{coolant}} > N > P_{\text{manifold}}$

←  
 More influence on  $X$   
 $N > T_{\text{coolant}} > P_{\text{manifold}}$

The trend shows that the intake manifold pressure has the minimum impact on fuel dynamics parameters and this mitigates the requirement for fuel compensation during intake pressure variations. Identified  $\Delta T$  for different operating conditions are indicated in Table 2.  $\Delta T$  decreases with either increasing engine speed or increasing intake manifold pressure. This is due to a higher exhaust gas velocity and a lower engine cycle time at higher engine speeds. A higher intake pressure also results in a higher exhaust pressure, which increases the exhaust gas velocity in the exhaust system. Table 2 indicates that changing the engine speed has a stronger impact on  $\Delta T$  compared with that of the intake pressure for the range studied.

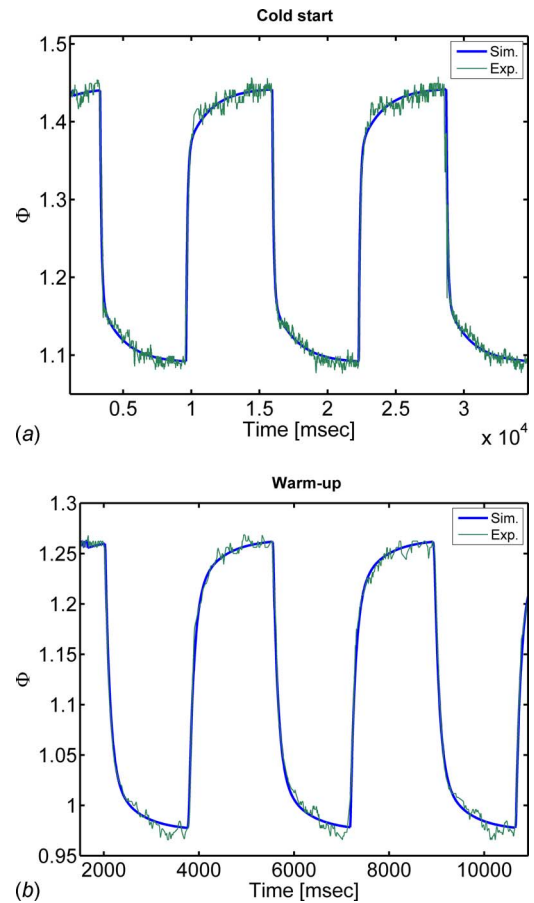


Fig. 2 Measured and simulated equivalence ratios for two different thermal test conditions: (a)  $T_{\text{coolant}} = -15^\circ\text{C}$ ,  $P_{\text{manifold}} = 50\text{ kPa}$  and (b)  $T_{\text{coolant}} = 45^\circ\text{C}$ ,  $P_{\text{manifold}} = 44\text{ kPa}$

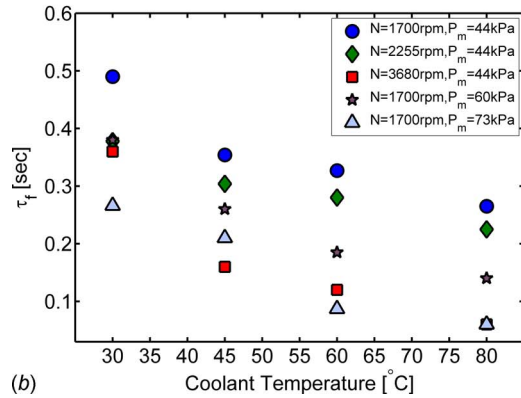
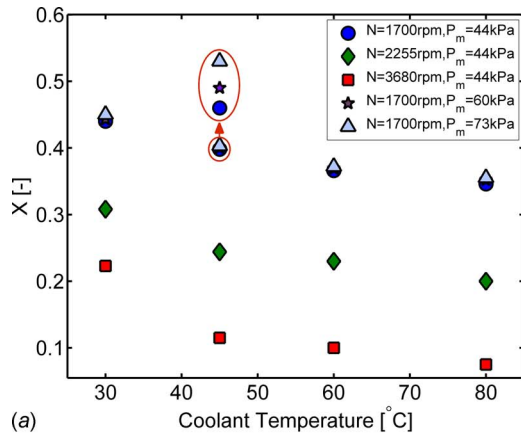


Fig. 3 Influence of coolant temperature, engine speed, and intake manifold pressure on fuel dynamics parameters in warm-up conditions

## 5 Fuel Dynamics Compensation

The prime purpose of this study is to estimate fuel dynamics parameters. However, the structure of a fuel dynamics compensator is briefly explained to indicate how the identified parameters from the fuel dynamics model can be used to control injected fuel in transient conditions. Proportional, integral (PI) controllers using feedback data from the AFR sensor are typically used to control AFR during steady-state operation. But these controllers are not capable of precise AFR control during transient conditions. A feed forward compensator is used to accomplish precise AFR control during transient conditions such as cold start and warm-up operations. For a proper control, the transfer function of the feed forward compensator is chosen as the inverse of the system dynamics ( $X$ - $\tau_f$  model) [17,27]

$$G_c = \frac{1 + \tau_f S}{1 + (1 - X)\tau_f S} \quad (5)$$

This lead compensator mainly affects transient response of the system and has no impact on steady-state response. Using Tustin approximation and  $z$ -inverse transform, the fuel dynamics compensator in a discrete form yields

$$\begin{aligned} \text{TIC}(k) = & \frac{2\tau_f + T}{2\varepsilon\tau_f + T} \text{TIB}(k) - \frac{2\tau_f - T}{2\varepsilon\tau_f + T} \text{TIB}(k-1) \\ & + \frac{2\varepsilon\tau_f - T}{2\varepsilon\tau_f + T} \text{TIC}(k-1), \quad \varepsilon = 1 - X \end{aligned} \quad (6)$$

where TIB and TIC are the injection pulse widths before and after compensation, respectively,  $T$  is the sampling period, and  $K$  is the sampling (injection) counter.

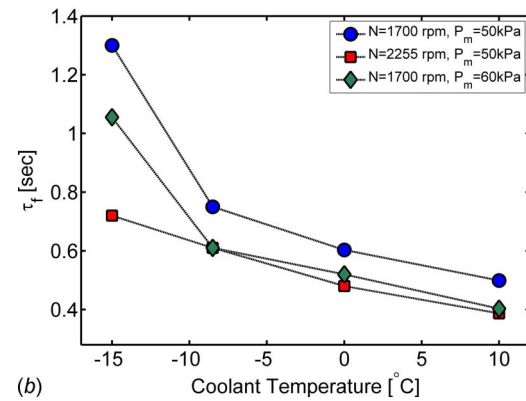
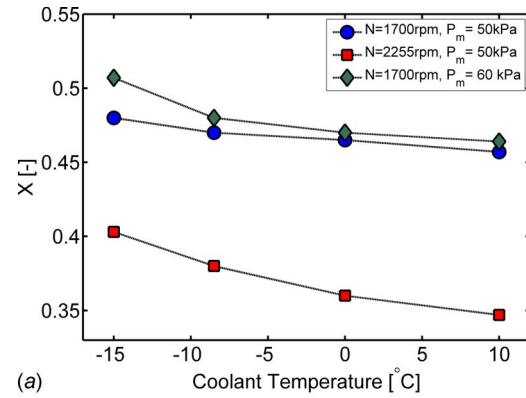


Fig. 4 Influence of coolant temperature, engine speed, and intake manifold pressure on fuel dynamics parameters in cold start conditions

In the case of a sudden throttle opening, air mass flow rate into the cylinder increases abruptly. To keep  $\Phi$  constant, injected fuel should be adjusted with consideration of dynamics in transporting fuel into the cylinder. Figure 5 indicates the performance of the model-based fuel dynamics compensator for transient operation at cold phase condition with a coolant temperature of  $-15^\circ\text{C}$  ( $X = 0.51$ ,  $\tau_f = 1.3$  s). Target  $\Phi$  in Fig. 5 is 1.2 and the cylinder input fuel mass flow rate should be 250 g/min to achieve the target  $\Phi$ . If no compensation of fuel dynamics is done and the fuel flow rate is only stepped up to obtain the target  $\Phi$ , the fuel mass flow rate follows the trend shown in Fig. 5 and it takes over 4 s to reach the target fuel mass flow rate. But the fuel injection based on the model-based compensator provides the target cylinder input fuel flow rate immediately after the transient occurs and this helps to achieve the target  $\Phi$  during the transient operation.

## 6 Conclusions

Parameters of fuel transport dynamics model have been estimated for over 50 different operating points at engine thermal conditions ranging from  $-15^\circ\text{C}$  to  $82^\circ\text{C}$ . The analysis of the results from this study is summarized as follows:

Table 2 Values of  $\Delta T$  at different engine speeds and intake manifold pressures

$N$ (rpm)	$P_{\text{manifold}}$ (kPa)			Engine cycle time (ms)
	44	60	73	
1700	230 ms	210 ms	190 ms	70.5
2255	160 ms	150 ms	140 ms	53
3680	100 ms	90 ms	80 ms	32.5



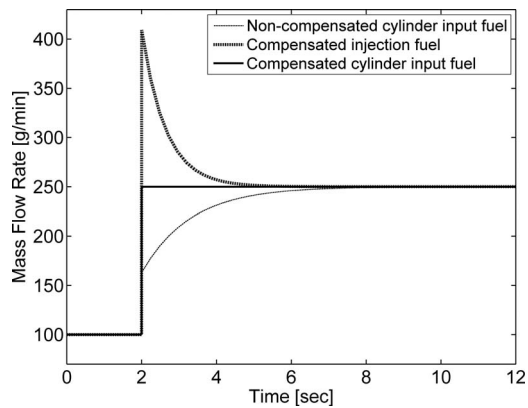


**Fig. 5 Model-based compensation for fuel dynamics during a transient at a cold phase operation ( $T_{\text{coolant}} = -15^{\circ}\text{C}$ )**

- Without requiring a costly cold chamber, the fuel dynamics parameters ( $X$  and  $\tau_f$ ) at cold start conditions can be determined for PFI engines, which use closed valve injection timing.
- Both  $X$  and  $\tau_f$  decrease with increasing coolant temperature. Similarly,  $\tau_f$  and  $X$  drop as the engine speed increases but  $X$  increases with increasing intake manifold pressure. However,  $\tau_f$  drops with an increase in the intake manifold pressure.
- The most effective parameter on  $\tau_f$  is the coolant temperature while the engine speed is the dominant parameter influencing  $X$ . Intake manifold pressure is found as the least influential parameter on  $\tau_f$  and  $X$ .
- The exhaust gas transport delay ( $\Delta T$ ) decreases with increasing engine speed or intake manifold pressure. In addition, the engine speed is found more influential on  $\Delta T$  compared to the effect of the intake pressure.
- A model-based feed forward fuel dynamics compensator can be applied to adjust fuel injection pulse width to obtain target AFR during transient conditions at cold start and warm-up conditions.

### Acknowledgment

The authors thank IPCO for providing financial support and giving permission to publish this work. IPCO's laboratory staff is gratefully acknowledged for close cooperation in the numerous experiments carried out.

### References

- [1] Li, H., Andrews, G. E., Savvidis, D., Daham, B., Ropkins, K., Bell, M., and Tate, J., 2008, "Study of Thermal Characteristics and Emissions During Cold Start Using an On-Board Measuring Method for Modern SI Car Real-World Urban Driving," SAE Paper No. 2008-01-1307.

- [2] Kyriakis, N. A., and Andre, M., 1998, "Cold Start of Passenger Cars," *Int. J. Veh. Des.*, **20**, pp. 137–146.
- [3] Shabbakhti, M., Jazayeri, S. A., Ghafuri, M., Aslami, A. R., Sahraeian, A., and Azadi, S., 2004, "A Novel Method to Estimate Parameters of the Wall-Wetting Fuel Model in MPFI Engines for Cold Start and Warm Up Conditions," ASME Internal Combustion Engine Technical Conference.
- [4] Rasmussen, I., 1971, "Emission fra Biler (Emissions From Cars)," Ph.D. thesis, Laboratory for Energetic, Technical University of Denmark, Lyngby, Denmark.
- [5] Aquino, C. F., 1981, "Transient A/F Control Characteristics of the 5 Liter Central Fuel Injection Engine," SAE Paper No. 810494.
- [6] Hires, S. D., and Overington, M. T., 1981, "Transient Mixture Strength Excursions—An Investigation of Their Causes and the Development of a Constant Mixture Strength Fuelling Strategy," SAE Paper No. 810495.
- [7] Cho, H., Min, K., Hwang, S.-H., and Lee, J.-H., 2000, "Prediction of the Air-Fuel Ratio in Transient Conditions Using a Model of Liquid Fuel Behavior in the Intake Port of a SI Engine," *Proc. Inst. Mech. Eng.*, **214**, pp. 731–740.
- [8] Curtis, E. W., Aquino, C. F., Trumpy, D. K., and Davis, G. C., 1996, "A New Port and Cylinder Wall Wetting Model to Predict Transient Air/Fuel Excursions in a Port Fuel Injected Engine," SAE Paper No. 961186.
- [9] Liand, J., and Collings, N., 1999, "A Semi-Empirical Model of Fuel Transport in Intake Manifolds of SI Engines and Its Application in Transient Conditions," SAE Paper No. 1999-01-1314.
- [10] Haluska, P., and Guzzella, L., 1998, "Control Oriented Modeling of Mixture Formation Phenomena in Multi Point Injection SI Gasoline Engines," SAE Paper No. 980628.
- [11] Neyachenko, I. I., 1998, "Method of A/F Control During SI Engine Cold Start," SAE Paper No. 981171.
- [12] Dodge, L. G., Leone, D. M., Shouse, K. R., Grogan, J., and Weeks, R. W., 1997, "Model Based Control and Cylinder-Event-Based Logic for an Ultra-Low Emissions Vehicle," SAE Paper No. 970531.
- [13] Lenz, U., and Schroeder, D., 1997, "Transient Air-Fuel Ratio Control Using Artificial Intelligence," SAE Paper No. 970618.
- [14] Berggren, P., and Perkovic, A., 1996, "Cylinder Individual Lambda Feedback Control in an SI Engine," M.Sc. thesis, Linköping University, Sweden.
- [15] Shaylor, P. J., Teo, Y. C., and Scarisbrick, A., 1995, "Fuel Transport Characteristics of Spark Ignition Engines for Transient Fuel Compensation," SAE Paper No. 950067.
- [16] Horie, K., Takahashi, H., and Akazaki, S., 1995, "Emission Reduction During Warm-Up Period by Incorporating a Wall-Wetting Fuel Model on the Fuel Injection Strategy During Engine Starting," SAE Paper No. 952478.
- [17] Almkvist, G., and Ericksson, S., 1994, "A Study of Air to Fuel Transient Response and Compensation With Different Fuels," SAE Paper No. 941931.
- [18] Hendricks, E., and Sorenson, S. C., 1990, "Mean Value Modeling of Spark Ignition Engines," SAE Paper No. 900616.
- [19] Chang, C.-F., Fekete, N. P., and Powell, J. D., 1993, "Engine Air-Fuel Ratio Control Using an Event-Based Observer," SAE Paper No. 930766.
- [20] Stefanopoulou, A. G., Cook, J. A., Grizzle, J. W., and Freudenberg, J. S., 1999, "Joint Air-Fuel Ratio and Torque Regulation Using Secondary Cylinder Air Flow Actuators," *ASME J. Dyn. Syst., Meas., Control*, **121**, pp. 638–647.
- [21] Chen, G., Asmus, T. W., and Weber, G. T., 1996, "Fuel Mixture Temperature Variations in the Intake Port," SAE Paper No. 961194.
- [22] Alkidas, A. C., 1994, "The Effects of Fuel Preparation on Hydrocarbon Emissions of a SI Engine Operating Under Steady-State Conditions," SAE Paper No. 941959.
- [23] Boam, D. J., Finlay, I. C., Biddulph, T. W., Ma, T. A., Lee, B., and Richardson, S. H., 1994, "The Sources of Unburned Hydrocarbon Emissions From Spark Ignition Engine During Cold Start and Warm Up," *Proc. Inst. Mech. Eng.*, Part A, **208**, pp. 1–11.
- [24] Cengel, Y., 1997, *Thermodynamics and Heat Transfer*, McGraw-Hill, New York.
- [25] Nelles, O., 2001, *Nonlinear System Identification*, Springer, Berlin.
- [26] Meyer, R., 1998, "Liquid Fuel Transport Into the Cylinder in Port Injected SI Engines," Ph.D. thesis, MIT, Cambridge, MA.
- [27] Kiencke, U., and Nielsen, L., 2000, *Automotive Control Systems*, Springer, Berlin.